

Pressure dependence of the reaction $\text{H} + \text{O}_2 (+\text{Ar}) \rightarrow \text{HO}_2 (+\text{Ar})$ in the range 1–900 bar and 300–700 K

J. Hahn,^a L. Krasnoperov,^b K. Luther^a and J. Troe^{*a}

^a *Institut für Physikalische Chemie, Universität Göttingen, Tammannstrasse 6, D-37077 Göttingen, Germany. E-mail: shoff@gwdg.de*

^b *New Jersey Institute of Technology, University Heights, Newark, NJ 07102-1982, USA*

Received 18th March 2004, Accepted 31st March 2004
First published as an Advance Article on the web 15th April 2004

The reaction $\text{H} + \text{O}_2 (+\text{Ar}) \rightarrow \text{HO}_2 (+\text{Ar})$ was studied in a high pressure flow cell in the bath gas argon at pressures between 1 and 900 bar and temperatures between 300 and 700 K. H atoms were generated by laser flash photolysis of NH_3 at 193.3 nm, HO_2 radicals were monitored by light absorption at 230 nm. The results are consistent with experimental low pressure rate constants $k_0 = [\text{Ar}] 2.5 \times 10^{-32} (T/300 \text{ K})^{-1.3} \text{ cm}^6 \text{ molecule}^{-2} \text{ s}^{-1}$ and theoretical high pressure rate constants $k_\infty = 9.5 \times 10^{-11} (T/300 \text{ K})^{+0.44} \text{ cm}^3 \text{ molecule}^{-1} \text{ s}^{-1}$ from the literature. The intermediate falloff curve was found to be best represented by $k/k_\infty = [x/(1+x)] F_{\text{cent}}^{1/(1+(a+\log x)^2/(N \pm \Delta N)^2)}$ with $x = k_0/k_\infty$, $a \approx 0.3$, $N \approx 1.05$, $\Delta N \approx 0.1$ ($+\Delta N$ for $(a + \log x) < 0$ and $-\Delta N$ for $(a + \log x) > 0$), and $F_{\text{cent}}(\text{Ar}) \approx 0.5$ independent of the temperature. A comparison with literature data between 300 and 1200 K does not confirm major deviations from third order kinetics in earlier medium pressure experiments.

1. Introduction

It is well known that the chain-terminating reaction



is of central importance in the oxidation of hydrogen-containing molecules. Its rate at low pressures has been measured repeatedly¹ since about 1945² and the uncertainty of the third order low pressure rate constant k_0 today is estimated to be about $\pm 25\%$. Investigations of a transition to the high pressure range of the reaction have been made only rarely. In experiments at 300 K up to pressures of 200 bar of the bath gas Ar the pseudo-second order rate constant k was found to fall about a factor of 10 below the extrapolated k_0 .³ Studies of the $\text{H}_2\text{-O}_2\text{-NO}_x$ reaction in Ar between 800 and 900 K and at pressures of 1–14 bar could not detect substantial deviations from third order.⁴ More recent shock tube measurements^{5,6} at Ar-pressures up to 110 bar and temperatures around 1300 K realized marked deviations from the third order low pressure limit. These experiments, however, were disputed⁷ on the basis of statistical adiabatic channel/classical trajectory (SACM/CT) predictions⁸ of the high pressure rate constant k_∞ combined with calculations of $k([\text{M}])$ in the falloff range of the reaction.⁹

The pressure dependence of the reaction may appear to be of only limited interest for normal combustion since deviations from third order occur only at comparably high pressures. However, because of the large importance of the reaction in combustion, even modest deviations may become relevant when precise rate constants are required. This is particularly true when the bath gas is a very efficient collider such as

water.⁶ There is considerable interest in the high pressure properties of the reaction in the field of supercritical water oxidation where temperatures are of the order of 800–1000 K and water pressures are around 250 bar.^{10–12} In order to decide the above mentioned dispute^{6,7} and to provide data for the construction of precise high temperature falloff curves, we have designed a new high pressure flow cell and investigated the reaction at pressures of the bath gas argon up to 900 bar and over the temperature range 300–700 K. These experiments now allow us to characterize the pressure dependence of the reaction up to temperatures such as they are of interest for combustion and supercritical water oxidation applications.

2. Experimental technique

Our high pressure flow cell was made from highly heat resistant stainless steel (Inconel alloy 718 from Special Metals Co.). The internal diameter of the cylindrical cell was 22 mm and its optical pathlength was 100 mm. The cell was closed with quartz windows of 20 mm thickness at both ends. Reaction mixtures were slowly flowing through the cell in such a way that the complete volume was exchanged between individual runs of the experiments. The cell could be heated up to 900 K at pressures up to 1000 bar, the temperatures in the cell were controlled by thermocouples. The reaction mixtures were preheated before flowing through the cell; gas temperatures in the cell were found to be constant within about 2%. Reaction mixtures consisting of 10^{-4} –1% of O_2 , 0.1–100 ppm of NH_3 and the bath gas Ar (99.9999%) were prepared in storage vessels and compressed by an oil-free membrane compressor.

H atoms were produced by laser flash photolysis of NH_3 using an ArF excimer laser at 193 nm. HO_2 radicals were monitored by light absorption at 230 nm using a high pressure Hg–Xe arc lamp as light source. Typically about 1000 runs were averaged. Rise times of the HO_2 signals of the order of 1 μs and decay times of the order of 15 μs were observed, see Fig. 1. The rise of the HO_2 signal was almost entirely dominated by the reaction $\text{H} + \text{O}_2 \rightarrow \text{HO}_2$ and it was only marginally influenced by secondary reactions which were modelled by a complete mechanism such as characterized by the data given in ref. 1. The HO_2 profile of Fig. 1 documents the quality of the signal and demonstrates the different time scales of the rise of the HO_2 concentration and its decrease due to loss processes. The pseudo-first-order rate constants for HO_2 formation were strictly proportional to the concentration of O_2 . More details of our experimental technique, the modelled mechanism and results for other bath gases such as helium and nitrogen will be described in a later publication.¹³ At this stage we only report the results obtained in argon because a

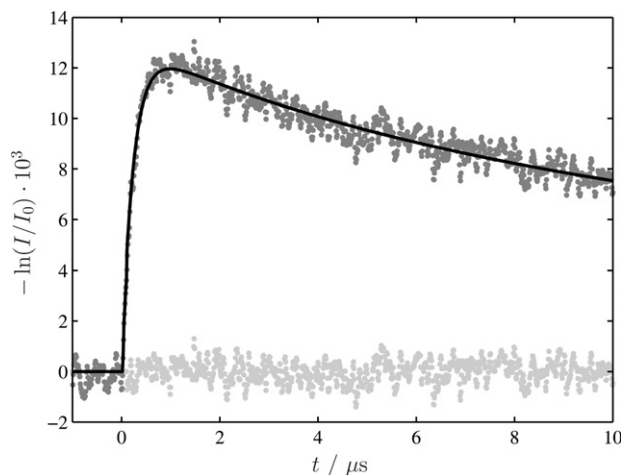


Fig. 1 HO₂ absorption signal at 230 nm ($T = 400$ K, $p = 900$ bar of Ar, full line = fit of the signal by detailed reaction mechanism; the horizontal trace is the residual of the fitted curve).

comparison with the high pressure measurements from refs. 3–6 can be made for this bath gas.

3. Results

Without tabulating the individual measured points in this communication, Fig. 2 summarizes our results in a doubly reduced falloff plot. k/k_∞ is shown as a function of k_0/k_∞ , employing the recommended experimental low pressure rate constant

$$k_0 = [\text{Ar}]2.5 \times 10^{-32} (T/300 \text{ K})^{-1.3} \text{ cm}^6 \text{ molecule}^{-2} \text{ s}^{-1} \quad (2)$$

from the evaluation in ref. 1, and the theoretical high pressure rate constant

$$k_\infty = 9.5 \times 10^{-11} (T/300 \text{ K})^{+0.44} \text{ cm}^3 \text{ molecule}^{-1} \text{ s}^{-1} \quad (3)$$

from ref. 8. The latter was calculated with an *ab initio* potential energy surface of HO₂ and employing an SACM/CT approach. The results of this treatment in refs. 14–16 were compared with calculations made on the DMBE IV potential energy surface¹⁷ and the expression for k_∞ given in eqn. (3) was confirmed. Fig. 2 indicates that a common reduced falloff plot can represent all data from 300 to 700 K. We found that the conventional¹⁸ symmetric falloff expression

$$\frac{k}{k_\infty} = \left(\frac{x}{1+x} \right) F_{\text{cent}}^{1/(1+(\log x)^2/N^2)} \quad (4)$$

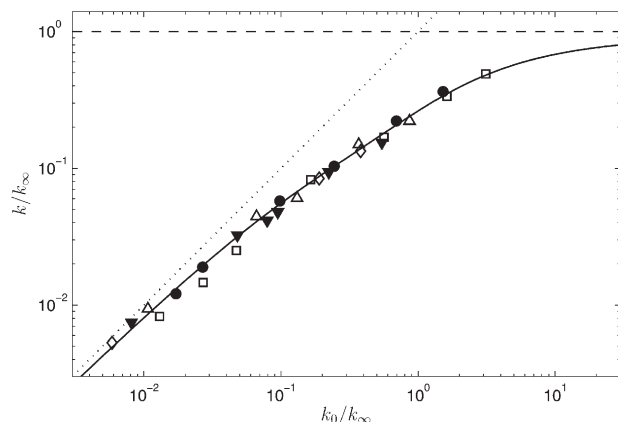


Fig. 2 Doubly reduced falloff curve of the reaction $\text{H} + \text{O}_2 (+\text{Ar}) \rightarrow \text{HO}_2 (+\text{Ar})$ (\square : 300 K, \bullet : 400 K, \triangle : 500 K, \blacktriangledown : 600 K, \diamond : 700 K, \cdots : k_0 , $---$: k_∞ , $—$: fit by eqn. (5)).

with $x = k_0/k_\infty$ and $N \approx 0.75 - \log F_{\text{cent}}$ did only provide a fair fit of the data from Fig. 2. Instead an asymmetric falloff expression^{9,19}

$$\frac{k}{k_\infty} = \left(\frac{x}{1+x} \right) F_{\text{cent}}^{1/(1+(a+\log x)^2/(N \pm \Delta N)^2)} \quad (5)$$

produced better agreement with the data and with the modelled falloff curves.⁹ This fit is included in Fig. 2 with the parameters $a \approx 0.3$, $N \approx 0.75 - \log F_{\text{cent}} \approx 1.05$, $\Delta N \approx 0.1$ ($+\Delta N$ for $(a + \log x) < 0$ and $-\Delta N$ for $(a + \log x) > 0$). The center broadening factor $F_{\text{cent}}(\text{Ar}) \approx 0.5$ as well as the parameters a and ΔN were found to be essentially independent of the temperature. Eqns. (2), (3), and (5) serve for the construction of full sets of falloff curves such as shown in Fig. 3. The agreement between the present results and the given expression, of course, is the result of fixing the fit parameters. One realizes that the experiments from ref. 4 correspond practically to the low pressure limit. The experiments from refs. 5 and 6, on the other hand, are found to be somewhat further into the transition range between k_0 and k_∞ . However, in agreement with the conclusions from ref. 6, one finds that the highest points from ref. 6 for some unknown technical reason are probably too low. One has to realize that the precision of the shock wave experiments was not good enough to provide precise information on the shape of the falloff curve such as this was possible in the present work. Nevertheless, it cannot be ruled out that complications, which were not considered in the theoretical modelling of ref. 9, at high temperatures lead to additional broadenings of the falloff curves. Such complications, *e.g.*, may arise from nonstatistical lifetime distributions of HO₂* such as suggested for H₂O₂* in ref. 20. However, unless such effects are clearly proven to exist, the falloff curves derived in the present work should be used in all practical applications.

4. Conclusions

The present experiments have provided strong experimental support for the previously modelled^{7–9} falloff curves of reaction (1) over wide ranges of temperatures and pressures. After accounting for different values of k_0 in different bath gases,¹ eqns. (2), (3), and (5) will provide an adequate basis for representing k in the fields of high pressure combustion and supercritical water oxidation.

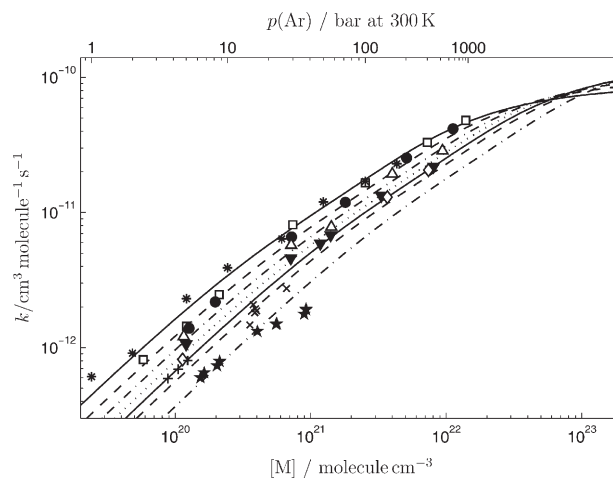


Fig. 3 Falloff curves of the reaction $\text{H} + \text{O}_2 (+\text{Ar}) \rightarrow \text{HO}_2 (+\text{Ar})$ (fitted curves from Fig. 2 for 300 K:—, 400 K:---, 500 K:---, 600 K:---, 700 K:---, 820 K:---, 1200 K:---, from left to right; experimental points: \star : ref. 6, \times : ref. 5, $+$: ref. 4, $*$: ref. 3, other points: this work with symbols from Fig. 2).

Acknowledgements

Financial support of this work by the Deutsche Forschungsgemeinschaft (SFB 357 "Molekulare Mechanismen unimolekularer Prozesse") is gratefully acknowledged.

References

- 1 D. L. Baulch, C. T. Bowman, C. J. Cobos, R. A. Cox, Th. Just, J. A. Kerr, M. J. Pilling, D. Stocker, J. Troe, W. Tsang, R. W. Walker and J. Warnatz, *J. Phys. Chem. Ref. Data*, 2004, **33**(Suppl. 2).
- 2 N. N. Semenov, *Acta Physicochim. URSS*, 1945, **20**, 291.
- 3 C. J. Cobos, H. Hippler and J. Troe, *J. Phys. Chem.*, 1985, **89**, 342.
- 4 M. A. Mueller, R. A. Yetter and F. L. Dryer, *Proc. Combust. Inst.*, 1998, **27**, 177.
- 5 D. F. Davidson, E. L. Petersen, M. Röhrig, R. K. Hanson and C. T. Bowman, *Proc. Combust. Inst.*, 1996, **26**, 481.
- 6 R. W. Bates, D. M. Golden, R. K. Hanson and C. T. Bowman, *Phys. Chem. Chem. Phys.*, 2001, **3**, 2337.
- 7 J. Troe, *Proc. Combust. Inst.*, 2000, **28**, 1463.
- 8 L. B. Harding, J. Troe and V. G. Ushakov, *Phys. Chem. Chem. Phys.*, 2000, **2**, 631.
- 9 J. Troe and V. G. Ushakov, *Faraday Discuss.*, 2001, **119**, 145.
- 10 H. R. Holgate and J. W. Tester, *Combust. Sci. Technol.*, 1993, **88**, 369.
- 11 M. Alkam, V. Pai, P. Butler and W. Pitz, *Combust. Flame*, 1996, **106**, 110.
- 12 E. E. Brock and P. E. Savage, *AIChE J.*, 1995, **41**, 1874.
- 13 J. Hahn, L. Krasnoperov, K. Luther and J. Troe, to be published.
- 14 J. M. C. Marques and A. J. C. Varandas, *Phys. Chem. Chem. Phys.*, 2001, **3**, 2632; J. M. C. Marques and A. J. C. Varandas, *Phys. Chem. Chem. Phys.*, 2001, **3**, 505.
- 15 L. B. Harding, J. Troe and V. G. Ushakov, *Phys. Chem. Chem. Phys.*, 2001, **3**, 2630.
- 16 L. B. Harding and J. Troe, *J. Chem. Phys.*, 2001, **115**, 3621.
- 17 M. R. Pastrana, L. A. M. Quintales, J. Brandão and A. J. C. Varandas, *J. Phys. Chem.*, 1990, **94**, 8073.
- 18 J. Troe, *J. Phys. Chem.*, 1979, **83**, 114.
- 19 J. Troe, *Ber. Bunsen-Ges. Phys. Chem.*, 1983, **87**, 161.
- 20 J. Troe and V. G. Ushakov, unpublished work.